

Synthetic Approaches for Accessing Rare-Earth Analogues of UiO-66

P. Rafael Donnarumma,^a Sahara Frojmovic,^a Paola Marino,^a Hudson A. Bicalho,^a Hatem M. Titi,^{a,b} Ashlee J. Howarth^{a*}

^aDepartment of Chemistry and Biochemistry, and Centre for NanoScience Research, Concordia University, 7141 Sherbrooke St W., Montréal, QC, H4B 1R6

^bDepartment of Chemistry, McGill University, 801 Sherbrooke St W., Montréal, QC, H3A 0B8

Supplementary information

S.1 Materials

All solvents and reagents were purchased from commercial sources. *N,N'*-dimethylformamide (DMF), *N,N*-dimethylacetamide (DMA), acetone, and nitric acid (70%) were purchased from Fisher Scientific (Fisher Chemical). $\text{Y}(\text{NO}_3)_3 \cdot 6\text{H}_2\text{O}$, $\text{Eu}(\text{NO}_3)_3 \cdot 6\text{H}_2\text{O}$, $\text{Gd}(\text{NO}_3)_3 \cdot x\text{H}_2\text{O}$, $\text{Tb}(\text{NO}_3)_3 \cdot x\text{H}_2\text{O}$, $\text{Ho}(\text{NO}_3)_3 \cdot x\text{H}_2\text{O}$, $\text{Er}(\text{NO}_3)_3 \cdot x\text{H}_2\text{O}$, $\text{Tm}(\text{NO}_3)_3 \cdot x\text{H}_2\text{O}$, and $\text{Yb}(\text{NO}_3)_3 \cdot x\text{H}_2\text{O}$ were purchased from Alfa Aesar. 2,6-difluorobenzoic acid (2,6-DFBA) was purchased from Combi-Blocks. Terephthalic acid (BDC) was purchased from Acros Organics. NMR solvents D_2SO_4 and DMSO-d_6 were purchased from Alfa Aesar. All solvents and chemicals were used without further treatment.

S.2 Instrumentation

Single crystal X-ray diffraction (SCXRD) data for Tm-UiO-66 was measured on a Bruker D8 Venture diffractometer equipped with a Photon 200 area detector, and μS microfocus X-ray source (Bruker AXS, $\text{CuK}\alpha$ source). Measurements were carried out at 253K. The crystal diffracted weakly at high angles. Structure solution was carried out using the SHELXTL package from Bruker.¹ The parameters were refined for all data by full-matrix-least-squares or F2 using SHELXL.² It should be noted that disordered molecules (water, DMA and dimethylammonium) in the MOF pores, which could not be reliably modelled using discrete atoms, were subtracted by SQUEEZE, using the PLATON software.³ All of the nonhydrogen atoms were refined with anisotropic thermal parameters. Hydrogen atoms were placed in calculated positions and allowed to ride on the carrier atoms. All hydrogen atom thermal parameters were constrained to ride on the carrier atom.

Powder X-ray diffraction (PXRD) patterns were collected on a Bruker D2 Phaser diffractometer (measurements made over a range of $4^\circ < 2\theta < 20^\circ$ in 0.02° step with a 0.200 s scanning speed) equipped with a LYNXEYE linear position sensitive detector (Bruker AXS, Madison, WI). Neat samples were smeared directly onto the silicon wafer of a proprietary low-zero background sample holder. Data was collected using a continuous coupled $\theta/2\theta$ scan with $\text{CuK}\alpha$ ($\lambda = 1.54178 \text{ \AA}$). No important reflections can be observed after $20^\circ 2\theta$ for all the samples.

Variable temperature (VT) PXRD patterns were collected on a Bruker D8 Advance diffractometer (measurement made over a range of $2^\circ < 2\theta < 40^\circ$ in 0.02° step with a 0.200 s scanning speed) equipped with a LYNXEYE linear position sensitive detector (Bruker AXS, Madison, WI). Neat samples were smeared directly onto the silicon wafer of a proprietary low-zero background sample holder. Data was collected using a continuous coupled $\theta/2\theta$ scan with Ni-filtered $\text{CuK}\alpha$ ($\lambda = 1.54178 \text{ \AA}$). The setup was

equipped with an Anton Paar CHC⁺ chamber. Diffractograms were collected in a stepwise fashion, and after each collection (ca. 7 min), the temperature in the chamber was raised in intervals of 5 °C at a rate of 1 °C min⁻¹ and a new collection started.

¹H-NMR spectra were recorded on a 300 MHz Bruker spectrometer and the chemical shifts were referenced to the residual solvent peaks.

Inductively coupled plasma – mass spectrometry (ICP-MS) data was measured on an Agilent 7500 Series.

Diffuse reflectance infrared spectra were recorded using a Thermo Scientific Nicolet 6700 FT-IR equipped with a MCT detector with a resolution of 1 cm⁻¹ in the range of 4000-450 cm⁻¹.

Thermogravimetric analysis (TGA) was carried out in a TGA/DSC 1 from Mettler Toledo, from room temperature to 800 °C at a rate of 5 °C/min under air.

Scanning electron microscopy (SEM) images were collected on a Phenom ProX desktop SEM.

MOF samples were activated using a Micromeritics SmartVacPrep instrument equipped with a hybrid turbo vacuum pump. Nitrogen adsorption-desorption isotherms were measured at 77K on a Micromeritics TriStar II Plus instrument.

S.3 Synthesis

RE-UiO-66 in DMF (RE = Y(III), Ho(III), Er(III), Tm(III), Yb(III)): Y-, Ho-, Er-, Tm- and Yb-UiO-66 were synthesised solvothermally in 6-dram vials containing the corresponding RE(NO₃)₃·xH₂O (0.174 mmol, assuming hexahydrate for all of them), BDC (28.5 mg, 0.171 mmol), and 2,6-DFBA (440 mg, 2.78 mmol), suspended in DMF (8 mL). The vials were sealed and placed into a preheated oven at 120 °C for 36 h. The precipitates were separated via centrifugation, washed three times with fresh DMF over the course of 24 h, and later three times with fresh acetone over the course of 24 h. The material was then air-dried and activated under vacuum at 80 °C, except for Ho-UiO-66.

RE-UiO-66 in DMF:DMA (RE = Eu(III), Gd(III), Tb(III)): Eu-, Gd-, Tb-UiO-66 were synthesised solvothermally in 6-dram vials containing the corresponding RE(NO₃)₃·xH₂O (0.174 mmol, assuming hexahydrate for both), BDC (28.5 mg, 0.171 mmol), and 2,6-DFBA (440 mg, 2.78 mmol), suspended in 8 mL of a DMA:DMF mixture with ratios of 7:1(Eu), 3:5(Gd) and 1:7(Tb). The vials were sealed and placed into a preheated oven at 120 °C for 48 h. The precipitates were separated via centrifugation, washed three times with fresh DMF over the course of 24 h, and later three times with fresh acetone over the course of 24 h. The material was then air-dried and activated under vacuum at 80 °C, except for Gd-UiO-66.

RE-UiO-66 in DMF with HNO₃ (RE = Y(III), Ho(III), Er(III), Tm(III), Yb(III)): Y-, Ho-, Er-, Tm- and Yb-UiO-66 were synthesised solvothermally in 6-dram vials containing the corresponding RE(NO₃)₃·xH₂O (0.174 mmol, assuming hexahydrate for all of them), BDC (28.5 mg, 0.171 mmol), 2,6-DFBA (440 mg, 2.78 mmol), concentrated HNO₃ (50 µL) suspended in DMF (8 mL). The vials were sealed and placed into a preheated oven at 120 °C for 36 h. The precipitates were separated via centrifugation, washed three times with fresh DMF over the course of 24 h, and later three times with fresh acetone over the course of 24 h. The material was then air-dried.

RE-UiO-66 in DMA (RE = Y(III), Eu(III), Gd(III), Tb(III), Ho(III), Er(III), Tm(III), Yb(III)): the RE-UiO-66 were synthesised solvothermally in 6-dram vials containing the corresponding RE(NO₃)₃·xH₂O (0.174 mmol, assuming hexahydrate for both), BDC (28.5 mg, 0.171 mmol), and 2,6-DFBA (440 mg, 2.78 mmol), suspended in DMA (8 mL). The vials were sealed and placed into a preheated oven at 120 °C for

72 h. The precipitates were separated via centrifugation, washed three times with fresh DMF over the course of 24 h, and later three times with fresh acetone over the course of 24 h. The material was then air-dried.

Tm-UiO-66 single crystals: single crystals of Tm-UiO-66 were synthesised solvothermally in 6-dram vials containing $\text{Tm}(\text{NO}_3)_3 \cdot x\text{H}_2\text{O}$ (0.087 mmol, assuming hexahydrate), BDC (14.3 mg, 0.085 mmol), 2,6-DFBA (220 mg, 1.39 mmol), HCl 35.5% (300 μL), in DMA (8 mL). The vials were sealed and placed into a preheated oven at 120 °C for 72 h. Octahedral crystals of approx. 80 μm crystals suitable for SCXRD were collected from the walls of the vial.

Some optimal ratios that can be used for a DMF:DMA mixture for the synthesis of RE-UiO-66 (RE = Y(III), Ho(III), Er(III), Tm(III) and Yb(III)) are 6:2 and 4:4, in case DMF alone does not give the expected product.

Zr-UiO-66 for reference was synthesised according to previously reported procedures.⁴

S.4 Diffuse reflectance infrared Fourier transform spectroscopy

Diffuse reflectance infrared Fourier transformed spectroscopy (DRIFTS) was used to confirm the presence of the carboxylate group from the linker. The samples were run after activation with no further treatment.

S.5 ¹H-NMR

~5 mg of activated sample was digested in D_2SO_4 and diluted with DMSO-d_6 . The digestion was carried on in a vial wherein the sample was attacked first with around 10 drops of D_2SO_4 and sonicated for 10 min. The slurry was then diluted with DMSO-d_6 and loaded into an NMR tube. This experiment was done only to confirm the presence of BDC in the structure of the synthesised material.

For identifying the cation, ~5 mg of activated sample was digested in a NaOH solution in D_2O (40% m/m) with sonication for 30 min. The final volume was brought up to 0.8 mL. The mixture was then centrifuged and the supernatant was loaded into an NMR tube.

S.6 ICP-MS

For ICP-MS, ~ 1 mg of the activated RE-UiO-66 (RE = Y(III), Tb(III), Er(III), Tm(III), Yb(III)) was weighed and digested in 750 μL H_2SO_4 at high temperatures in a sand bath for 24 h. This solution is diluted with deionised H_2O to a final volume of 10 mL. Finally, an aliquot of this solution is diluted by 50 times and injected in the equipment. Calculations were done assuming the following formula for the activated sample: $[(\text{CH}_3)_2\text{NH}_2]_2[\text{RE}_6(\text{OH})_8(\text{BDC})_6]$. A higher experimental percentage of metal in the material than theoretical percentage is indicative of the presence of linker defects in the structure.

S.7 TGA

For TGA analysis, ~ 5 mg of the activated RE-UiO-66 (RE = Y(III), Eu(III), Tb(III), Er(III), Tm(III), Yb(III)) was weighed with no further treatment. The final percentage of the RE_2O_3 residue is adjusted for the presence of humidity below 100 °C and then compared to the expected value for the perfect formula, $[(\text{CH}_3)_2\text{NH}_2]_2[\text{RE}_6(\text{OH})_8(\text{BDC})_6]$. Figure S8.1 shows the procedure use to estimate the experimental percentage. A higher experimental percentage RE_2O_3 than the expected value is indicative of the presence of missing linkers.

S.8 Zr₆ and RE₆ Secondary Building Unit

The metal node in Zr-UiO-66 can be defined as: $Zr_6(\mu_3-OH)_4(\mu_3-O)_4(COO^-)_{12}$, giving a net neutral charge: $(+4)*6 + (-1)*4 + (-2)*4 + (-1)*12 = 0$

As a result, there is no need for any charge compensating ions in Zr-UiO-66, or similar structures containing metals with oxidation state IV. The same is not true for RE(III)-based hexanuclear clusters, wherein the building block can be defined as $RE_6(\mu_3-OH)_{8-x}(\mu_3-O)_x(COO^-)_{12}^{y-}$, for a 12-connected structure such as RE-UiO-66 (or other 12-connected structures reported in the literature).⁵ In this case, x is assigned so as to minimise the charge in the framework as much as possible. The charge is brought to its minimum within the framework when $x = 0$

$$(+3)*6 + (-1)*8 + (-2)*0 + (-2)*6 = -2.$$

Bridging -OH groups are confirmed using DRIFTS (Figure S12) and the presence of DMA cations to balance the charge is confirmed by NMR (Figure S10) on an acetone exchanged and activated sample. Previous reports of similar structures define the cluster in the same way.^{5,6}

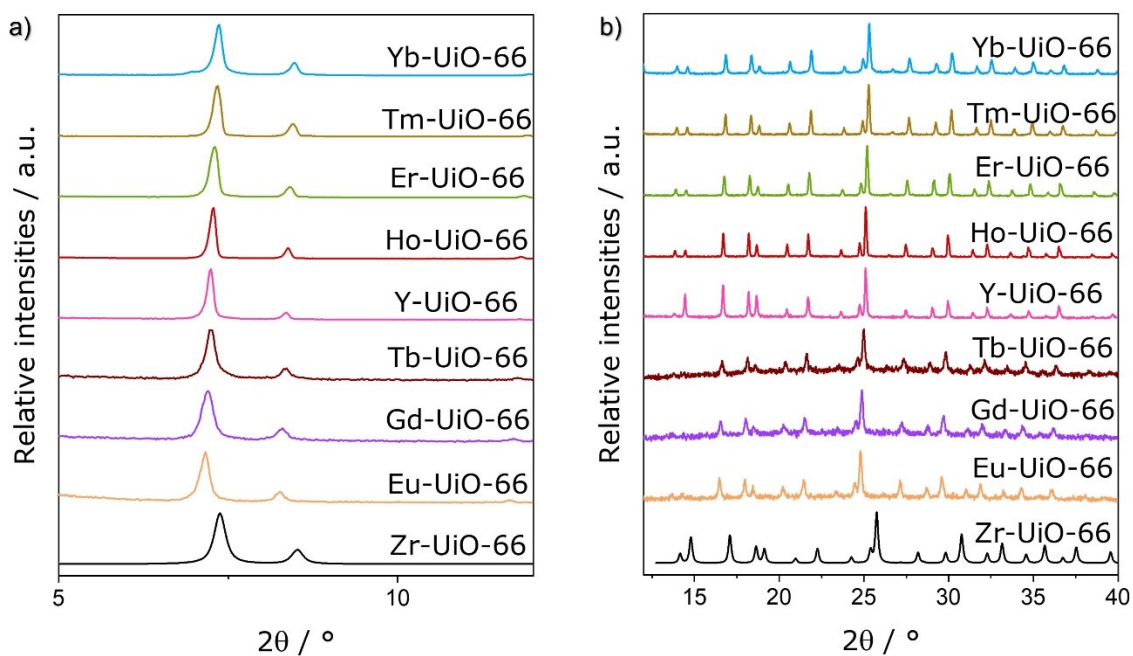


Figure S1 Stacked PXRDs for all the RE-UiO-66 analogues, and Zr-UiO-66 for comparison from (a) 5 to 12 °2θ and (b) 12 to 40 °2θ.

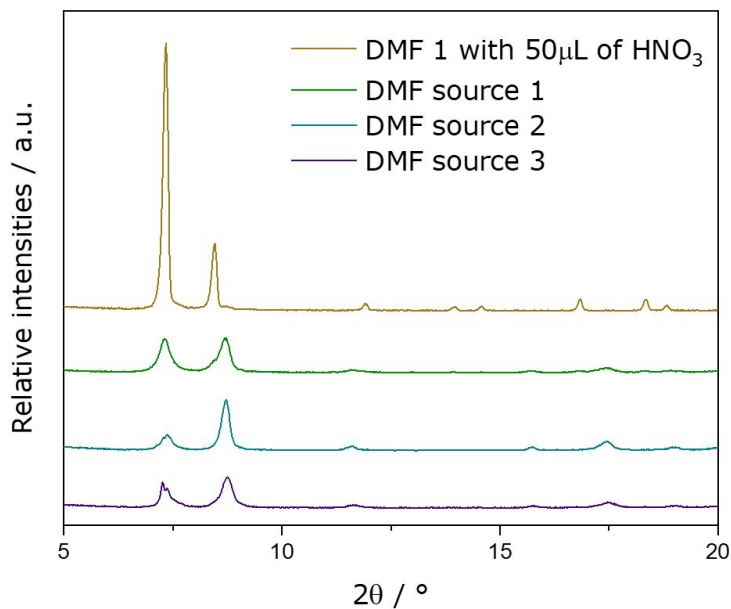


Figure S2 Stacked PXRD patterns showing the product of the synthesis in DMF for the as-synthesised Tm-UiO-66. The bottom three patterns are not the desired product. Upon the addition of HNO₃ to the synthesis, Tm-UiO-66 is obtained (top).

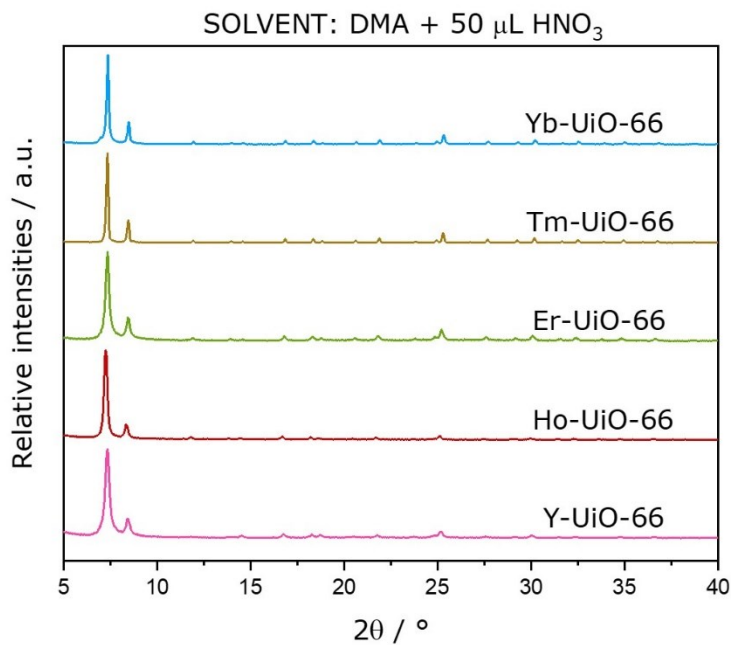


Figure S3 Stacked PXRD patterns showing the product of the synthesis in DMF with HNO₃ for as-synthesised RE-UiO-66 (RE = Y(III), Ho(III), Er(III), Tm(III), Yb(III)).

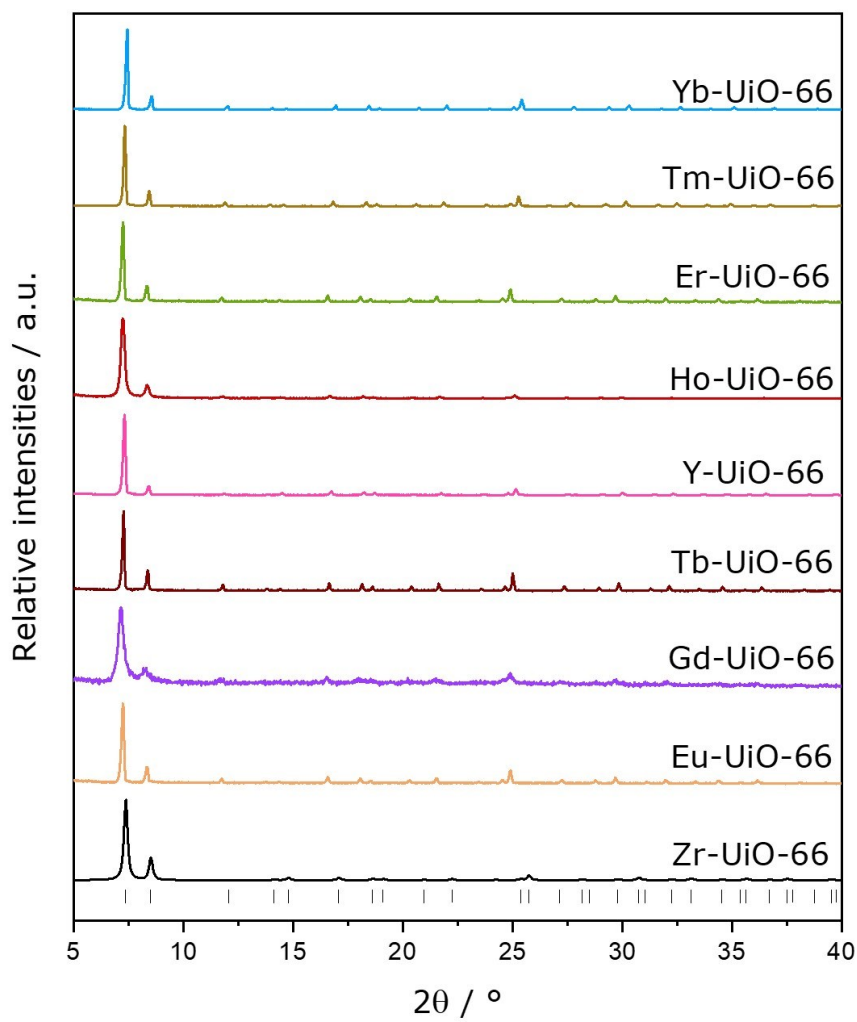


Figure S4 Stacked PXRD patterns showing the product of the synthesis in DMA for RE-UiO-66 (RE = Eu(III), Gd(III), Tb(III), Y(III), Ho(III), Er(III), Tm(III), Yb(III)). Zr-UiO-66 can be found at the bottom for comparison. Vertical lines are the allowed reflections from the Tm-UiO-66 crystal structure.

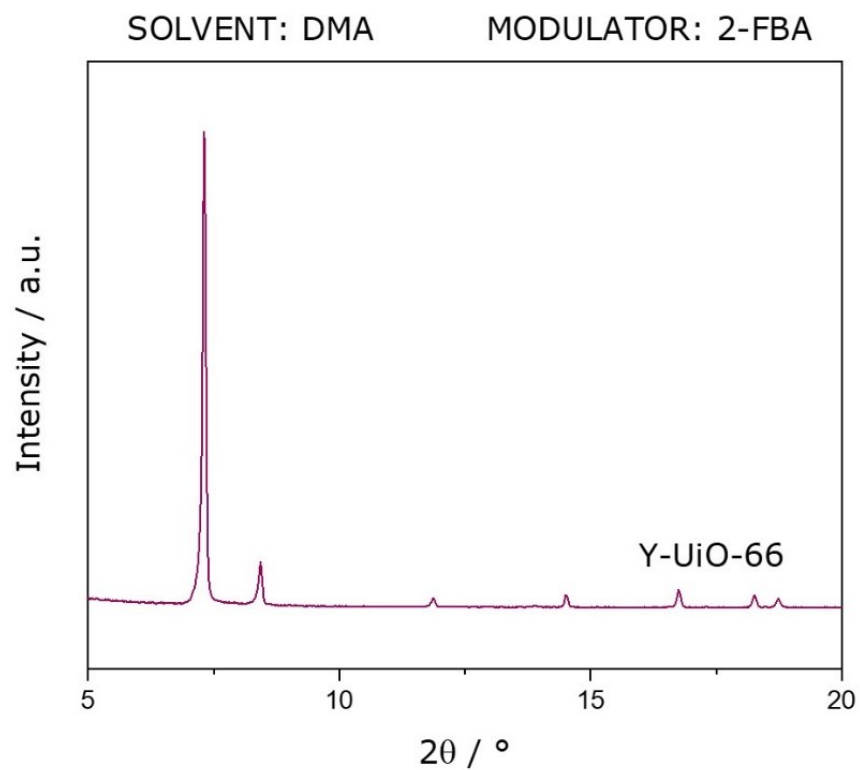


Figure S5 PXRD of Y-Uio-66 synthesised in DMA with 2-FBA as the modulator.

Table S1 Activation conditions attempted for Y-Uio-66.

Temperature (°C)	Time (h)	Surface area (m ² /g)
150	24	1060
130	24	1350
120	24	1350
80	20	1370

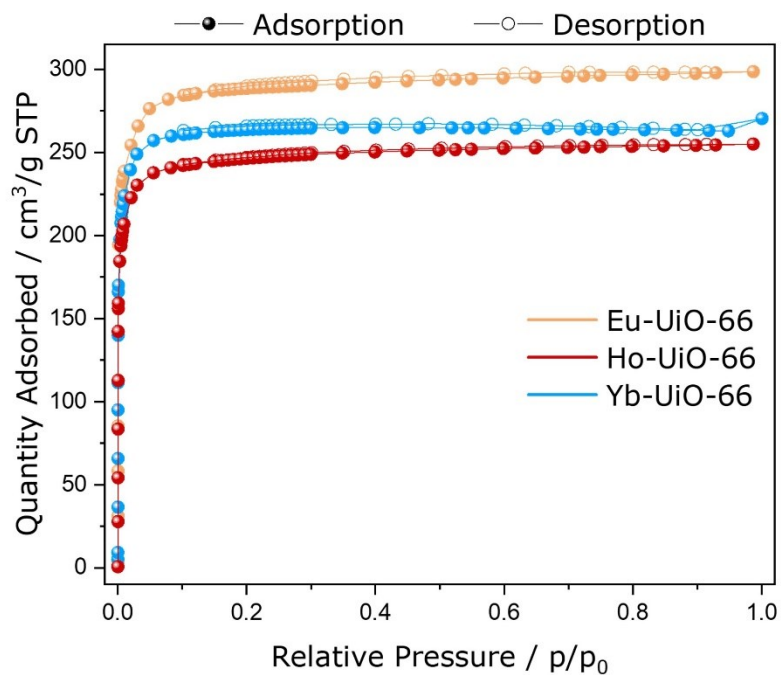


Figure S6. Nitrogen adsorption-desorption isotherms for RE-UiO-66 (RE = Eu(III), Ho(III), Yb(III)). Isotherms for RE = Y(III), Gd(III), Tb(III), Er(III), Tm(III) are represented in Fig. 3.

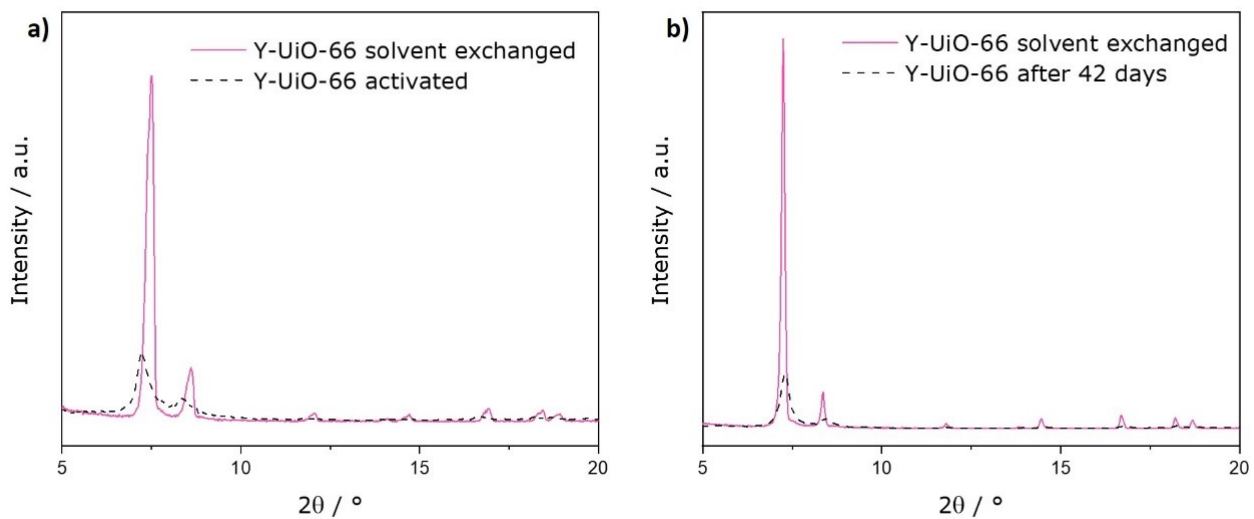


Figure S7. PXRD patterns showing loss of crystallinity of Y-UiO-66 (a) after activation, and (b) when sitting in the vial air-exposed for 42 days.

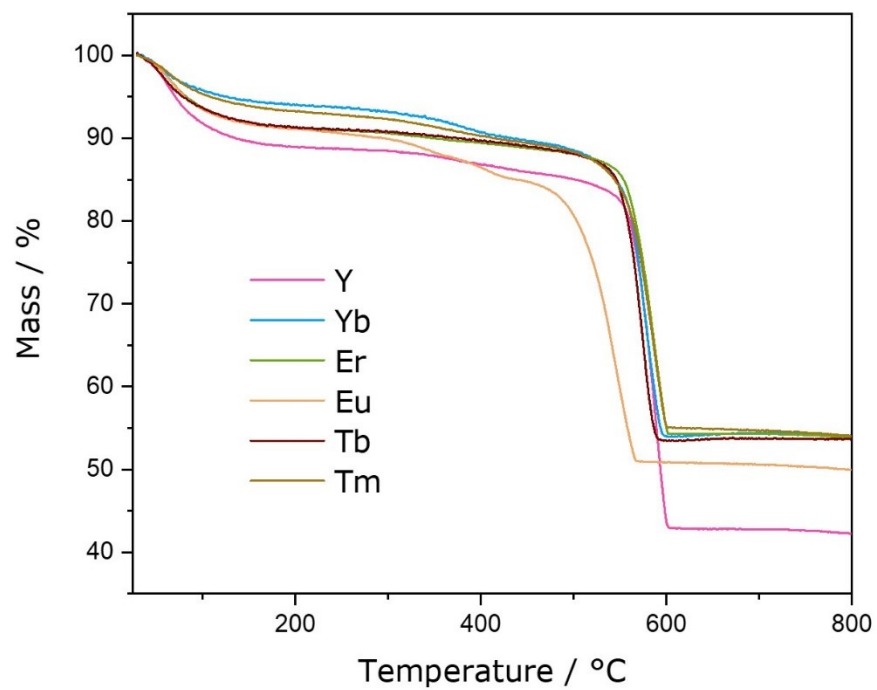


Figure S8 TGA plots for RE-UiO-66 (RE = Y(III), Yb(III), Er(III), Eu(III), Tb(III), Tm(III)).

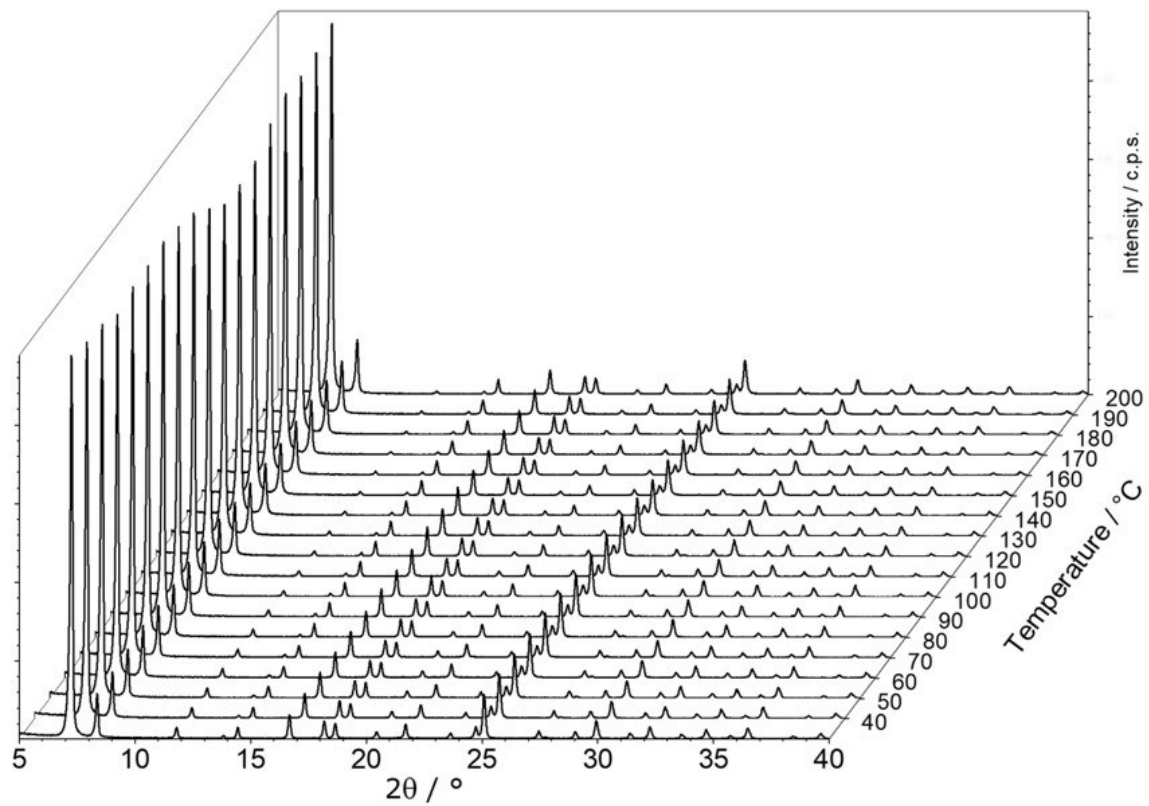


Figure S9 VT-PXRD of Y-Uio-66 from 25 °C to 200 °C.

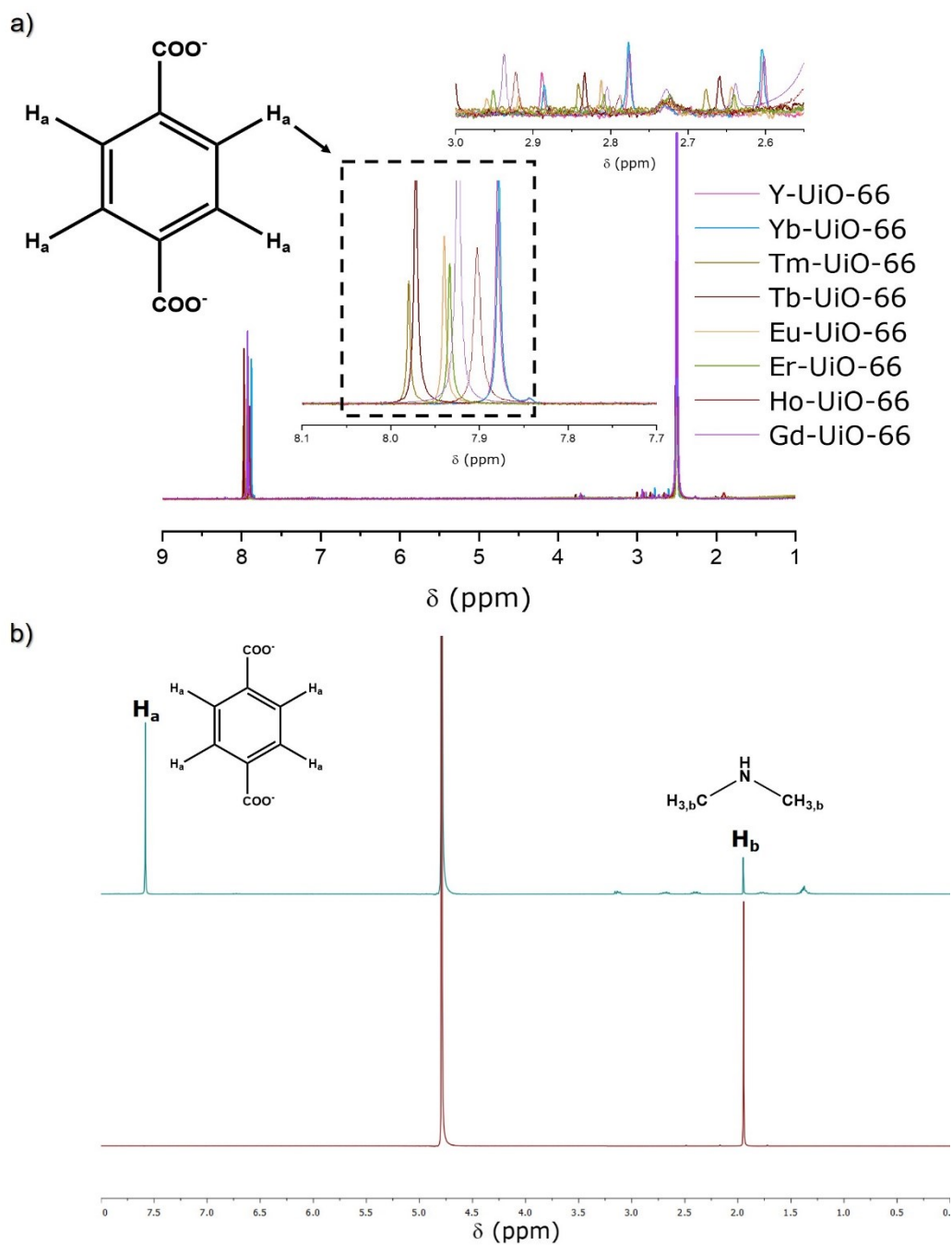


Figure S10 ^1H -NMR spectrum for (a) RE-UiO-66 (RE = Y(III), Yb(III), Tm(III), Tb(III), Eu(III), Er(III), Ho(III), Gd(III)) digested in D_2SO_4 and solubilized in DMSO-d_6 , differences in chemical shift might be due to varying amounts of deuterated sulfuric acid changing solvent polarity; (b) Y-UiO-66 (top) and $(\text{CH}_3)_2\text{NH}\cdot\text{HCl}$ (bottom) digested in a mixture of D_2O and NaOH .

Table S2 ICP values for the RE-UiO-66 (except Eu).

RE	%RE theoretical	%RE ICP
Y	30.55	32.47
Tb	44.02	49.65
Er	44.99	48.43
Tm	45.53	50.44
Yb	46.12	46.93

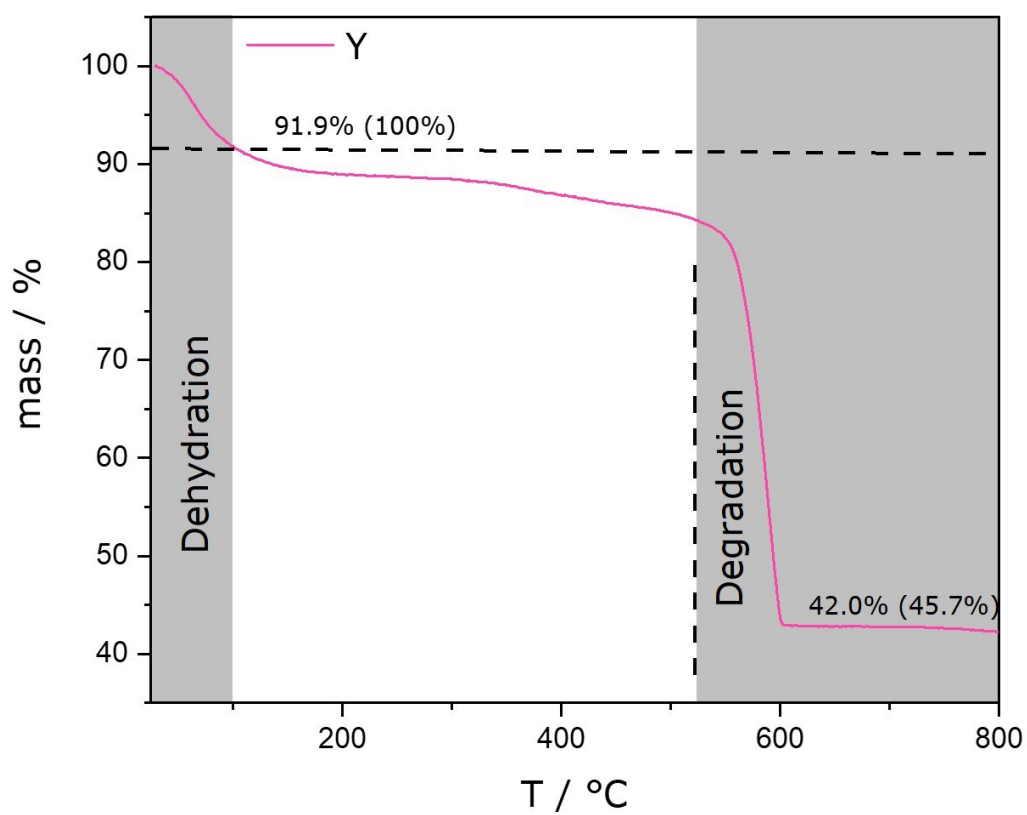


Figure S11 TGA plot for Y-UiO-66 detailing how the experimental Y₂O₃ percentage is estimated.

Table S3 TGA %_{REoxide} for RE-UiO-66.

RE	% _{REoxide} theoretical	% _{REoxide} TGA
Y	38.8	45.7
Eu	49.7	55.2
Tb	50.7	57.0
Er	51.5	57.2
Tm	52.0	57.6
Yb	52.5	56.6

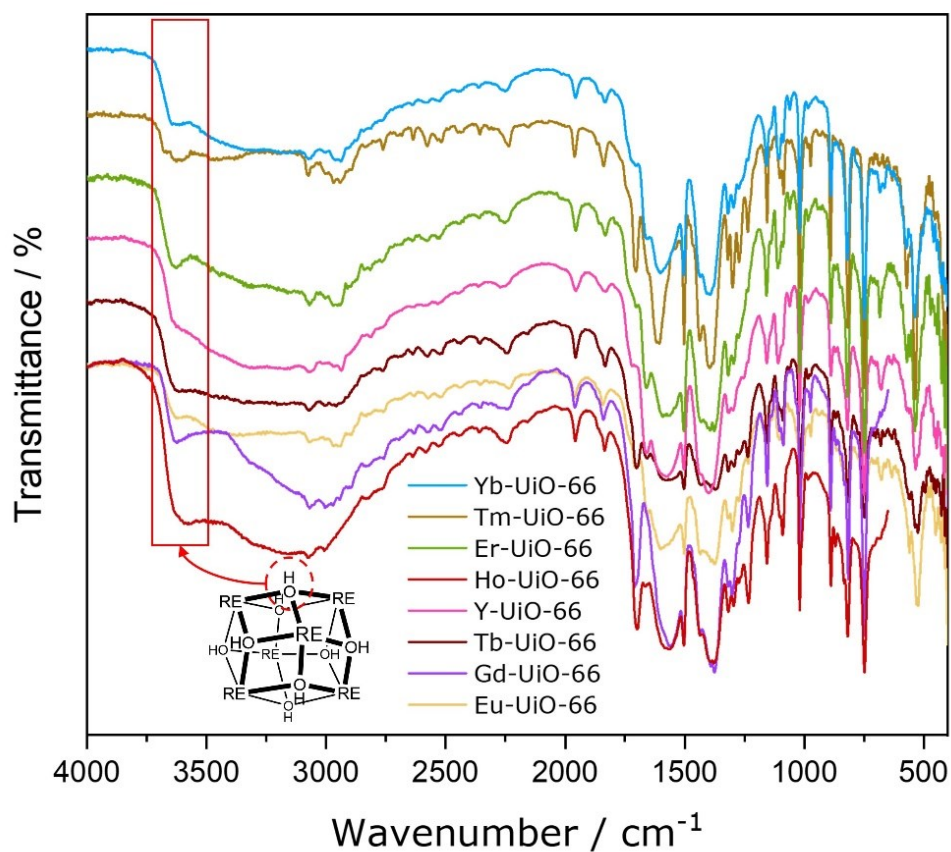


Figure S12 DRIFTS spectra for RE-UiO-66 (RE = Yb(III), Tm(III), Er(III), Ho(III), Y(III), Tb(III), Gd(III), Eu(III)). All materials show similar peaks, confirming that they are all isostructural. O-H stretch band from cluster is highlighted. Spectra are stacked for clarity.

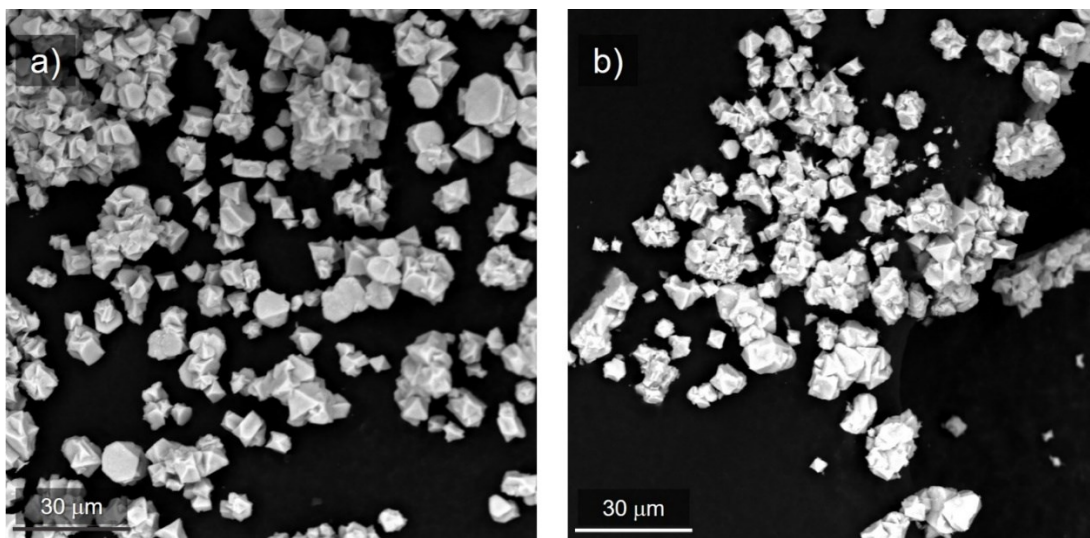


Figure S13 SEM of (a) Yb-UiO-66 and (b) Er-UiO-66. Octahedral shapes can be distinguished in the images.

S.8 Crystallographic data

184 e⁻ were squeezed from the structure due to an impossibility to solve the molecules in the pores due to the high level of disorder. To this point the structure was solved yielding the following formula: Tm₃(OH)₄(BDC)₃. This framework is anionic, and its charge needs to be countered with a counterion. (CH₃)₂NH₂⁺ is the only possible present counterion needed to balance the charge so, 26 e⁻ have to belong to it. The remaining 158 e⁻ are assigned to 3 DMA molecules (48e⁻ each) and 1.5 H₂O molecules (10 e⁻ each). The final formula for this compound ends up being would then be [(CH₃)₂NH₂]₁[Tm₃(OH)₄(BDC)₃·(DMA)₃·(H₂O)_{1.5}].

Empirical formula	C ₂₄ H ₁₂ O ₁₆ Tm ₃
Formula weight	1062.13
Temperature/K	253(2)
Crystal system	Cubic
Space group	<i>Fm</i> $\bar{3}$ <i>m</i>
a/Å	21.2553(16)
b/Å	21.2553(16)
c/Å	21.2553(16)
α /°	90
β /°	90
γ /°	90
Volume/ Å ³	9603(2)
Z	8
ρ_{calc} /g/cm ³	1.471
μ /mm ⁻¹	10.408
F(000)	3928.0
2 θ range for data collection/°	7.204 to 144.87
Index ranges	-26<=h<=26 -26<=k<=26 -26<=l<=26
Reflections collected	43503
Independent reflections	539 [Rint = 0.1137, Rsigma = 0.0208]
Data/restraints/parameters	539/12/27
Goodness-of-fit on F ²	1.173
Final R indexes [I>=2 σ (I)]	R1 = 0.0369, wR2 = 0.0950
Final R indexes [all data]	R ₁ = 0.0433, wR ₂ = 0.1065
Largest diff. peak/hole / e Å ⁻³	1.09/-1.08



Figure S14 Asymmetric unit of Tm-UiO-66.

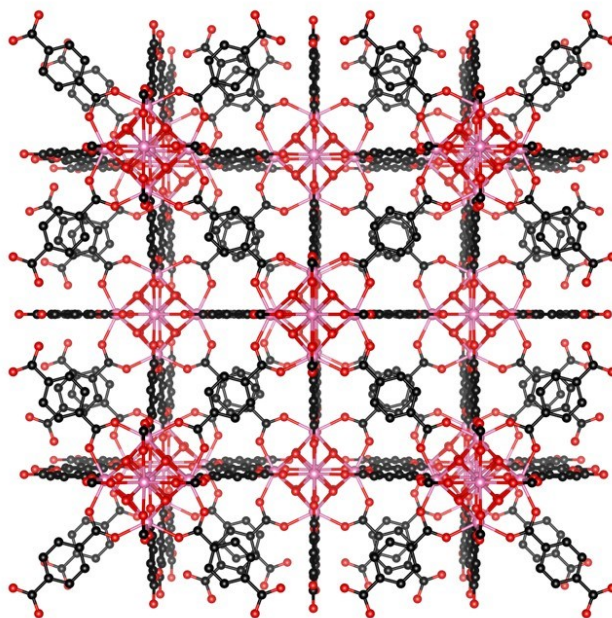


Figure S15 Overall representation of Tm-UiO-66 framework (empty pores).

All MOF structure figures were prepared using VESTA 3.⁷

S.9 References

1. G. M. Sheldrick, *Acta Cryst. C.*, 2015, **C71**, 3–8.
2. G. M. Sheldrick, *Acta Cryst. A.*, 2015, **A71**, 3–8.
3. A. L. Spek, *Acta Cryst. C.*, 2015, **C71**, 9– 18.
4. M. J. Katz, Z. J. Brown, Y. J. Colón, P. W. Siu, K. A. Scheidt, R. Q. Snurr, J. T. Hupp, O. K. Farha, 2013, *Chem. Commun.*, **49**, 9449-9451.
5. R. Luebke, Y. Belmabkhout, Ł. J. Weseliński, A. J. Cairns, M. Alkordi, G. Norton, Ł. Wojtas, K. Adila, M. Eddaoudi, 2015, *Chem. Sci.*, **6**, 4095-4102. (b) C. Liu, S. V. Eliseeva, T.-Y. Luo, P. F. Muldoon, S. Petoud, N. L. Rosi, 2018, *Chem. Sci.*, **9**, 8099-8102.
6. A. H. Assen, Y. Belmabkhout, K. Adil, P. M. Bhatt, D.-X. Xue, H. Jiang, M. Eddaoudi, 2015, *Angew. Chem. Int. Ed.*, **54**, 14353-14358
7. K. Momma and F. Izumi, *J. Appl. Crystallogr.*, 2011, **44**, 1272 -1276